1202 82 anil. no team by 28, 2021

Unraveling different chemical fingerprints between a champagne wine and its aerosols

Gérard Liger-Belair^{a,1}, Clara Cilindre^a, Régis D. Gougeon^b, Marianna Lucio^c, Istvan Gebefügi^c, Philippe Jeandet^a, and Philippe Schmitt-Kopplin^{c,1}

^aLaboratoire d'Oenologie et Chimie Appliquée, Unité de Recherche Vigne et Vins de Champagne-Unité Propre de Recherche et de l'Enseignement Supérieur EA 2069, Université de Reims Champagne-Ardenne, BP 1039, 51687 Reims, France; ^bInstitut Universitaire de la Vigne et du Vin–Jules Guyot, EA 581 EMMA, Université de Bourgogne, 21078 Dijon, France; and ^cInstitute for Ecological Chemistry, BioGeoChemistry, and Analytics, Helmoltz Zentrum München, Ingoldstädter Landstraße 1 D-85764 Neuherberg, Germany

Edited by Jerrold Meinwald, Cornell University, Ithaca, NY, and approved August 13, 2009 (received for review June 12, 2009)

As champagne or sparkling wine is poured into a glass, the myriad of ascending bubbles collapse and radiate a multitude of tiny droplets above the free surface into the form of very characteristic and refreshing aerosols. Ultrahigh-resolution MS was used as a nontargeted approach to discriminate hundreds of surface active compounds that are preferentially partitioning in champagne aerosols; thus, unraveling different chemical fingerprints between the champagne bulk and its aerosols. Based on accurate exact mass analysis and database search, tens of these compounds overconcentrating in champagne aerosols were unambiguously discriminated and assigned to compounds showing organoleptic interest or being aromas precursors. By drawing a parallel between the fizz of the ocean and the fizz in Champagne wines, our results closely link bursting bubbles and flavor release; thus, supporting the idea that rising and collapsing bubbles act as a continuous paternoster lift for aromas in every glass of champagne.

Fourier transform | ion cyclotron resonance | MS | bubbles | surfactants

In surfactant solutions, preferential adsorption of surfactants at the air-solution interface occurs as a result of the amphiphilic properties of surfactants, with the water-soluble moiety plunging into the solution and the hydrophobic component in contact with the air. In oceanography, enrichment of the sea-surface microlayer and atmospheric aerosols in surfactant materials has long been studied (1–3). Actually, bubbles trapped by the sea breakers action considerably increase exchange surfaces between the sea bulk and the atmosphere. Bubbles drag surfactants along their way through the liquid bulk, reach the sea surface, to finally burst and eject aerosol droplets into the atmosphere. Air bubbles trapped during rough sea conditions were found to increase specific organic concentrations in marine aerosols by several orders of magnitude compared with those found in the liquid bulk (4).

From a conceptual point of view, the situation found in glasses poured with champagne or sparkling wine is quite similar to that described above. Nevertheless, only quite recently, the tools of physical chemistry were used to identify the physical mechanisms behind the nucleation, rise, and collapse of bubbles found in champagne and sparkling wines (5–7). From a strictly chemical point of view, Champagne and sparkling wines are multicomponent hydro-alcoholic solutions supersaturated with CO₂dissolved gas molecules (formed together with ethanol during the fermentation process). Champagne and sparkling wines also hold hundreds of surface active compounds, some of them showing organoleptic interest. As soon as a bottle of champagne or sparkling wine is uncorked, the progressive release of CO₂dissolved gas molecules is responsible for bubble nucleation, the so-called effervescence process. It is worth noting that ≈5 L of CO₂ must escape from a typical 0.75 L champagne bottle. To get an idea of how many bubbles are potentially involved all along the degassing process, we can divide this volume of CO₂ to be released by the average volume of a typical bubble of 0.5 mm in

diameter. A huge number close to 108 is found, leading to an exchange surface ≈80 m². Once champagne is poured into a glass, bubbles nucleated on the glass wall drag champagne surfactants along their way through the liquid bulk (6, 7). Surfactants finally reach the free surface and concentrate themselves at the air/champagne interface. At the free surface of a glass poured with champagne, the ever-increasing concentration of surfactants was indeed indirectly evidenced by observing the ever-increasing lifetime of bubbles with time (7). Actually, the ever-increasing surface concentration of surfactants progressively changes the boundary conditions on the bubble surface from slip to nonslip; thus, reducing in turn the drainage velocity and extending the lifetime of the bubble. The formation of adsorption layers of amphiphile macromolecules at the air/ champagne interface was also directly evidenced through ellipsometry and Brewster angle microscopy (BAM) experiments (8, 9). Actually, bubbles bursting at the champagne surface radiate hundreds of tiny liquid jets every second, which quickly break up into a multitude of tiny droplets, as shown by use of high-speed photography, and laser tomography techniques very recently (Fig. 1) (5, 10). Based on a phenomenological analogy between the fizz of the ocean and the fizz in Champagne wines, it was hypothesized a few years ago that aerosols found in the headspace above a glass poured with champagne could considerably enhance the fragrance release of champagne by bringing chemical compounds to the taster's nostrils, showing both surface activity and organoleptic interest (7, 11). In the present work, an experimental proof is given using ultrahigh-resolution MS (Fourier Transform Ion Cyclotron Resonance Mass Spectrometer; FT-ICR-MS) as a nontargeted approach, to discriminate hundreds of surface active compounds, some of them showing indeed organoleptic interest, that are preferentially partitioning in champagne aerosols rather than in the champagne bulk. Thus, aerosols appear to hold the organoleptic essence of champagne.

Results and Discussion

Describing the Chemical Spaces of Both Champagne Bulk and Aerosols. Ultrahigh-resolution is the key in enabling the direct mass spectrometric comparison of bulk and aerosol spectra without need of absolute quantification. The combined advantages of the high mass accuracy (<200 ppb) and mass resolution (>500,000

Author contributions: G.L.-B., R.D.G., and P.S.-K. designed research; G.L.-B., C.C., R.D.G., I.G., and P.S.-K. performed research; M.L. contributed new reagents/analytic tools; C.C., R.D.G., M.L., I.G., P.J., and P.S.-K. analyzed data; and G.L.-B., C.C., R.D.G., P.J., and P.S.-K. wrote the paper.

The authors declare no conflict of interest.

This article is a PNAS Direct Submission.

Freely available online through the PNAS open access option.

¹To whom correspondence may be addressed. E-mail: gerard.liger-belair@univ-reims.fr or schmitt-kopplin@helmholtz-muenchen.de.

This article contains supporting information online at www.pnas.org/cgi/content/full/ 0906483106/DCSupplemental.

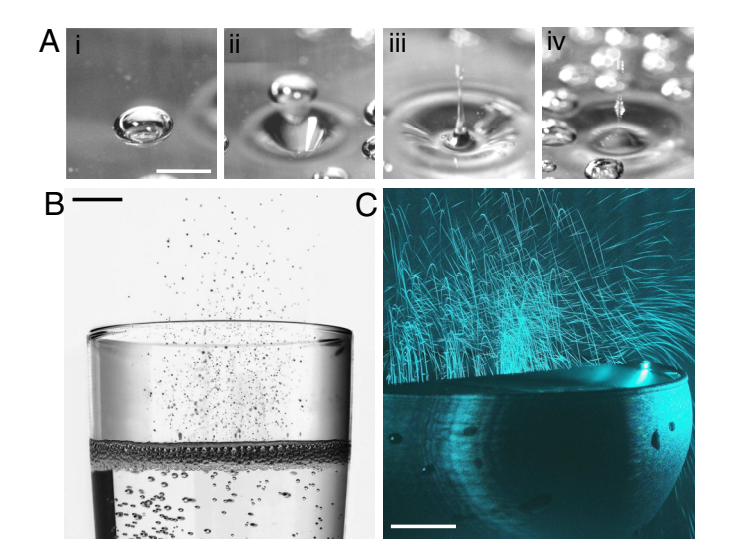


Fig. 1. Aerosois production above the free surface of a glass poured with champagne, as evidenced through high-speed photography and laser tomography techniques. (A) Reconstructed time-sequence showing four steps of the collapse of a single champagne bubble, by use of high-speed photography (11); the time interval between successive frames is ≈1 ms. (Scale bar, 1 mm.) [Reproduced with permission from ref.11 (Copyright 2001, American Society for Enology and Viticulture).] (B) While collapsing together, the myriad of bubbles literally skim off the upper layer found at the air/champagne interface into the form of hundreds of tiny droplets ejected every second up to several centimeters above the free surface (photograph by Alain Cornu/ collection CIVC). (Scale bar, 1 cm.) (C) Champagne aerosols found above the free surface of a glass, as seen through laser tomography techniques (5, 10). (Scale bar, 1 cm.) [Reproduced with permission from ref. 5 (Copyright 2008, The Royal Society of Chemistry).]

at m/z 300) make it possible to detect relative changes in signal intensity that can directly be related to changes in the concentration of compounds of known elemental composition. Also, the approach relies on the relative intensity change in signals within similar signal patterns and, thus, does not need any quantitative approach (not possible anyway when collecting the jets due to uncontrollable desolvation). The signal profiles were qualitatively compared by intensity ratio analysis of all masses found in the aerosol spectrum versus the champagne bulk spectrum.

For champagne aerosols, as well as for the champagne bulk, overall mass spectra in the mass range 150-1,000 were qualitatively very similar, with comparable signal profiles in many nominal masses (Fig. 2). Nevertheless, FT-ICR-MS enables a direct comparison of the signals within a mass window through a peak intensity ratio analysis providing a concentration factor denoted $C_{\rm f} = I_{\rm aerosols}/I_{\rm bulk}$ (Fig. 3). Signals being concentrated together during sampling or diluted during the collection would all have similar relative peak profiles and C_f over the mass range; thus, signals with relative higher intensity in aerosols can be clearly identified from the mass spectra (for example, as illustrated with masses 253, 227, and 225 in Fig. 4). Only some hundred signals, among the thousands found in the mass range 150–1,000, showed relative intensity increase in aerosols, such as the signal at m/z 253.2172, for example, corresponding to the $[C_{16}H_{29}O_2]^-$ ion. The other signals in nominal mass 253 corresponding to components [C₈H₁₃O₉]⁻ and [C₉H₁₇O₆S]⁻ experience no relative intensity variation in each given spectrum, as seen in Fig. 4A. An interpretation of such compilations of masses is made after assignment of elemental compositions with 2D van Krevelen diagrams (12, 13). Van Krevelen diagrams enable a structural visualization of ultrahigh-resolution mass spectra in their converted elemental compositions (i.e., plots of H/C versus

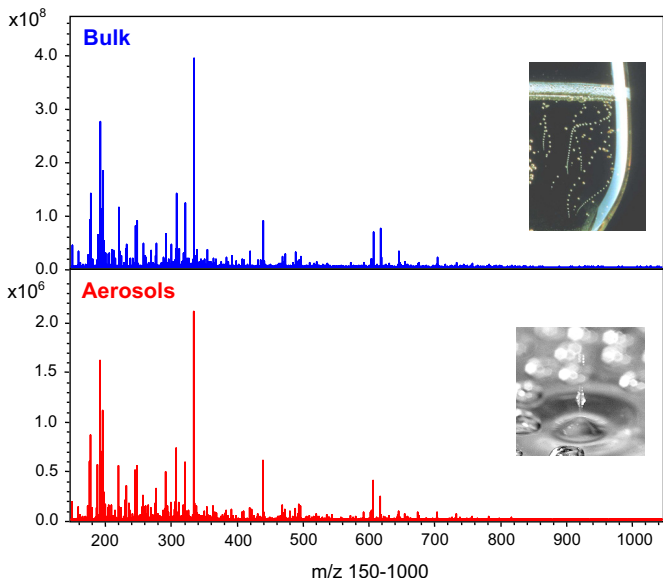


Fig. 2. Mass spectra of the champagne bulk and aerosols, respectively, showing the overall similarity of the spectra in the whole mass range m/z 150–1,000.

O/C, and H/C versus m/z, for each peak identified in the mass range 150 to 1,000). Hundreds of masses characteristic of the bulk and the aerosols, displayed in Fig. 5, provide a clear visual representation of the molecular partitioning that occurs at the air/champagne interface. In the different CHO, CHOS, CHON, and CHONS chemical spaces, 747 m/z signals with masses ranging from m/z 150 to 1,000 (Fig. 5A) can be assigned to unique absolute formulas, with 200 ppb tolerance and confirmation with ¹³C-signal. These formulas, which cover the nearly entire metabolome region of the van Krevelen diagram between 0 and 1 (O/C) and 0.5 and 2 (H/C) for the bulk (Fig. 5C), illustrate the high diversity of molecules detected under our negative electrospray ionization (ESI) conditions, which include, among others polyphenolics, amino acids, peptides, and fatty acids (14). As can be seen from Fig. 5 B and D, although in much lower quantities, molecules from each of the same different chemical spaces are also present in aerosols at higher concentrations than in the bulk. Nevertheless, when considering concentration factors $(C_f) > 2$, most of molecules that are specifically observed in champagne aerosols have m/z values between 150 and 450, as can be seen in Fig. 5B. Also, most of the molecules showing a $C_f > 2$ appear in

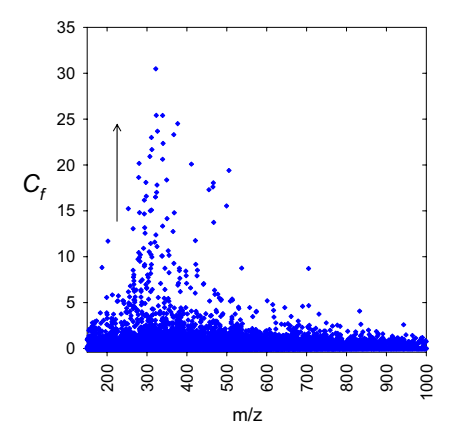


Fig. 3. Concentration factors analysis of all masses present in the mass spectra of champagne aerosols and bulk, respectively.

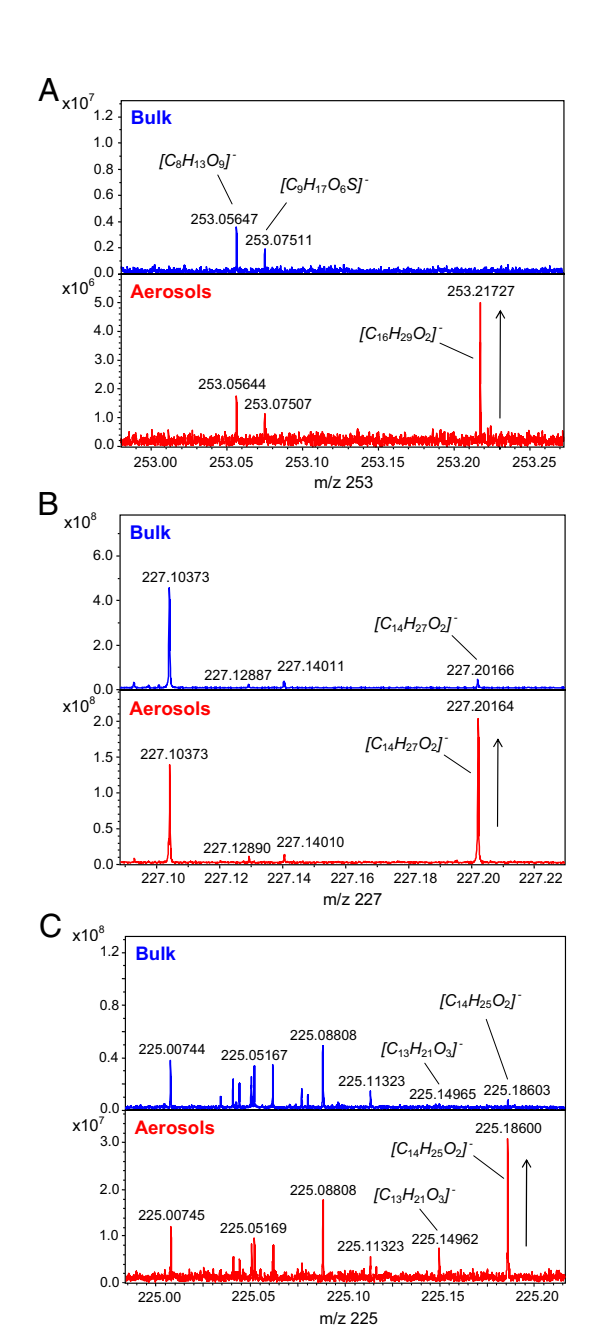


Fig. 4. Comparison of both bulk and aerosois mass spectra within three distinct mass windows. (*A*) Representative increase in peak intensity of mass 253.2172, assigned to $[C_{16}H_{29}O_2]^-$, relative to other signals in nominal mass 253. (*B*) Representative increase in peak intensity of mass 227.2016, assigned to $[C_{14}H_{27}O_2]^-$, relative to other signals in nominal mass 227. (*C*) Representative increase in peak intensity of masses 225.1496 and 225.1860, assigned respectively to $[C_{13}H_{21}O_3]^-$ and $[C_{14}H_{25}O_2]^-$, relative to other signals in nominal mass 225.

the upper left side of the van Krevelen diagrams (Fig. 5D), a region which, in the CHO chemical space, corresponds to saturated aliphatic structures of low oxygen content present in wines, which are very well-known to exhibit surfactant properties, such as fatty acids for example (15). However, valuable clues for the structural identification of some of these compounds are provided by topic related available databases such as KEGG, accessible with the MassTRIX interface (16), or SciFinder Scholar (Chemical Abstract Services, American Chemical Society, available at http://www.cas.org/SCIFINDER/SCHOLAR/).

Rising and Collapsing Bubbles Act As a Continuous Paternoster Lift for Aromas. Processing the 163 exact masses corresponding to the ionised species that are significantly more concentrated in champagne aerosols than in the bulk gives 32 and 13 possible metabolites present in different annotated Vitis vinifera and Saccharomyces cerevisiae organisms pathways, respectively, which are both relevant to wine biochemistry (Table S1). Among all these possible structures, and consistently with the van Krevelen diagrams of Fig. 5D, we can observe a remarkable nearly complete series of saturated fatty acid structures ranging from the C10 (decanoic) to the C24 (tetracosanoic), which come either from the yeast metabolism or directly from the grape (17, 18). Likewise, unsaturated fatty acids (UFAs) in C14:1 (myristoleic), C16:1 (palmitoleic), C18:1 (oleic), and in C18:2 (linoleic) are also reliable assumptions for compounds with surfactant properties, which are likely to be pulled out of the champagne bulk. Most interestingly, for each of the absolute formulas to which saturated fatty acids with the same number of carbons have been assigned in ESI(-), alternative structural isomers could be ethyl esters that needed to be confirmed in ESI(+), some of them being well-known to participate to the aroma of wine (19). For example, the neutral formula $C_{16}H_{32}O_2$, obtained from the peak at m/z 255.2329 in ESI(-) corresponding to the $[M-H]^-$ ion with absolute ion mass formula $[C_{16}H_{31}O_2]^-$, and which likely corresponds to palmitic acid, can also be assigned from the peak observed at m/z 257.2475 in ESI(+) to the ethyl tetradecanoate ester (ethyl miristate) $[C_{16}H_{33}O_2]^+$ (Table S1). Similarly, the $[C_{16}H_{29}O_2]^-$ ion observed in ESI(-) (Fig. 4A) can witness to the presence of the palmitoleic acid, whereas its corresponding [C₁₆H₃₁O₂]⁺ positive ion would relate to a propenoic acid, methyl, dodecyl ester (Table S1). It is worth noting that short chained esters (<C₁₄) were not found in the analyzed samples in ESI(+), but only their corresponding neutral isobaric acids in ESI(-). For example, the peak at m/z 227.2016 corresponding to the [M-H] ion with absolute mass formula $[C_{14}H_{27}O_2]^-$ can be found in the fatty acid biosynthesis pathway of V. vinifera as the tetradecanoic acid (Table S1). Similarly, because no isobaric ester was found in ESI(+), the $[C_{10}H_{19}O_2]^{-}$ ion can be attributed to decanoic acid only, which is known to exhibit acid and toasty aromas in Champagne wines (20). Another medium chain saturated fatty acid was identified at m/z199.1703 as dodecanoic acid, responsible for dry and metallic

A group of three mono (M)UFAs was also concentrated in Champagne aerosols. Indeed, we consistently assigned myristoleic acid to the $[C_{14}H_{25}O_2]^-$ ion at m/z 225.1860. Two other MUFAs, characterized as markers of foam quality of cavas (15), were identified at m/z 253.2172 and 281.2486 as palmitoleic acid and oleic acid, respectively. Then, a polyunsaturated fatty acid, namely linoleic acid, was assigned to m/z 279.2329. These unsaturated fatty acids constitute the main lipid fraction of grapes (18), and are also precursors of C6 compounds (22), responsible for herbaceous aromas.

Another important family of odorant compounds, namely norisoprenoids, is also likely to be overconcentrated in droplets as indicated by the peak at m/z 225.1496, which can be unambiguously assigned to the $[C_{13}H_{21}O_3]^-$ ion. A thorough survey of the literature using SciFinder Scholar indeed shows that the corresponding neutral formula relates to different isomers of odorant molecules reported as β -damascenone precursors (http://www.cas.org/SCIFINDER/SCHOLAR/). The latter can be for example isomers of dihydrovomofiliol or Blumenol B and Annuionone G, contributing to the fruity aroma of several grape varieties and related wines such as Syrah (23), Chardonnay (24), and Melon (25). Convincingly, an alternative isomer also corresponds to a related odorant norisoprenoid structure (dihydromethyl jasmonate) found in old English grape varieties (26). A further relevant compound was also possibly identified at m/z

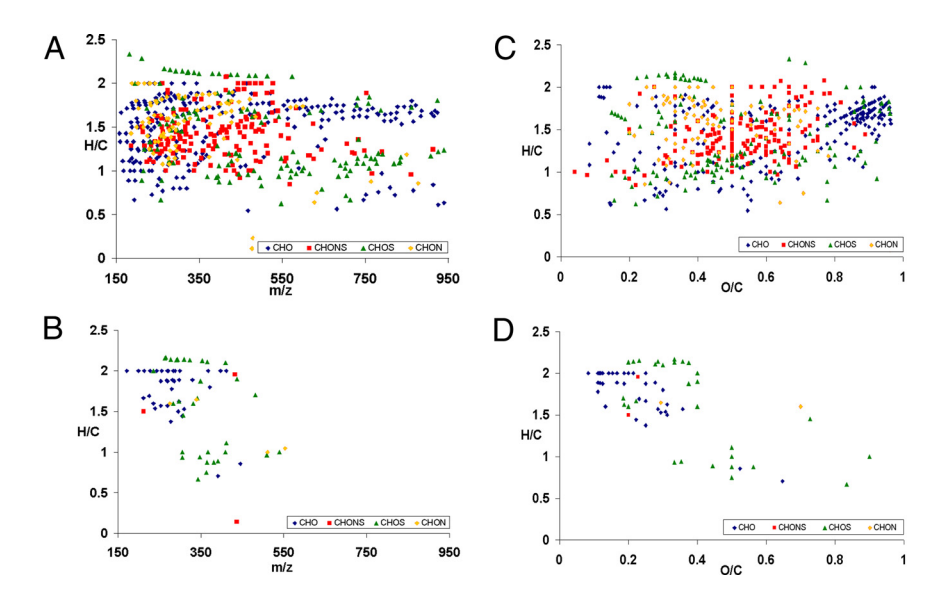


Fig. 5. Van Krevelen diagrams of the bulk showing the presence of typical CHO, CHOS, CHON, and CHONS wine metabolites in the m/z range 150 to 500 and higher molecular weight carbohydrates (A and C); Van Krevelen diagrams of molecules concentrated in the aerosols only (with $C_f > 2$) showing mainly CHO and CHOS highly saturated molecules with relative low oxygen contents (B and D). Color code: blue, CHO; green, CHOS; orange, CHON; red, CHONS.

297.2435 as ricinoleic acid (Table S1). Indeed, Pagot et al. (27) showed that peroxisomal β-oxidation of ricinoleic acid leads to γ-decalactone, a peachy aroma compound. Two other elemental formulas could be related to terpenoid glucose esters at m/z 325.2024 and 345.1556 (28). The latter is a glucose ester of (E)-2,6-dimethyl-6-hydroxyocta-2,7-dienoic acid and was previously detected in Riesling wine (29). Picrocrocin could correspond to the $[C_{16}H_{25}O_7]^-$ ionic elemental formula identified at m/z 329.1605. This molecule is a glucoside of safranal and contributes to the bitter taste of saffron (30). Last, two alternative isomers at m/z 171.1390 could correspond to monoterpene alcohols, which are considered as important aromas of wines from the Muscat grape variety (31).

In conclusion, we were interested in describing changes in the chemical complexity and diversity in champagne aerosols formation through ultrahigh-resolution MS, in the mass range 150–1,000. We were able to discriminate hundreds of chemical components that are preferentially partitioning in champagne aerosols rather than in the champagne bulk and could propose structural assignments for tens of them. By drawing a parallel between the fizz of the ocean and the fizz in Champagne wines, our study evidenced a relationship between bursting bubbles and the likely "exhausting aromas" effect often attributed to Champagne wines; thus, supporting the idea that rising and collapsing bubbles act as a continuous paternoster lift for aromas in every glass of champagne.

- Barger WR, Garret WD (1970) Surface-active organic material in the marine atmosphere. J Geophys Res 75:4561–4566.
- Mukerjee P, Handa T (1981) Adsorption of fluorocarbon and hydrocarbon surfactants to air-water, hexane-water, and perfluorohexane-water interfaces: Relative affinities and fluorocarbon-hydrocarbon nonideality effects. J Phys Chem 85:2298– 2303.
- Oppo C, et al. (1999) Surfactant components of marine organic matter as agents for biogeochemical fractionation and pollutant transport via marine aerosols. Mar Chem 63:235–253.
- O'Dowd C, De Leeuw G (2007) Marine aerosol production: A review of the current knowledge. Phil Trans R Soc A 365:1753–1774.
- Liger-Belair G, Polidori G, Jeandet P (2008) Recent advances in the science of champagne bubbles. Chem Soc Rev 37:2490–2511.
- Liger-Belair G, Jeandet P (2003) More on the surface state of expanding champagne bubbles rising at intermediate Reynolds and high Peclet numbers. Langmuir 19:801– 808
- 7. Liger-Belair G (2003) The science of bubbly. Sci Am 288:80-85.

Materials and Methods

Champagne Bulk Sampling. A standard Champagne wine was used for this set of experiments. Champagne was poured into glasses first thoroughly washed and rinsed by use of methanol. The champagne bulk was sampled directly from glasses, after champagne was poured. Samples were diluted 40 μ L/mL in methanol before flow injection in the FT-ICR-MS.

Champagne Aerosols Sampling. Microscope glass slides, also previously washed with methanol, were positioned at the top of glasses, 2 to 5 mm above the free surface of champagne. Champagne aerosols, originating from the myriad of bubbles collapsing at the air/champagne interface, progressively collect themselves by colliding the microscope glass slides. After 10 min of aerosols collection above champagne glasses, the slides were washed with methanol needy for flow injection in the FT-ICR-MS. Depending on the sampling time and the amount of methanol needed for elution from the slides, the final concentration infused was different and uncontrollable due to relative evaporation on the glass slide surface.

FT-ICR-MS Analysis. Ultrahigh-resolution mass spectra were carried out on a Bruker APEX Qe FT-ICR-MS equipped with a 12 Tesla superconducting magnet and an Apollo II ESI source operated with 1,000 scan (1 MW) in the positive ion mode and 500 to 5,000 scan (4 MW) in the negative mode. Mass scan range was 150–2,000 m/z for both modes. Spectra were externally calibrated on clusters of arginine (10 mg/L in methanol) and internally systematically on fatty acids [ESI(-)] and solvent diesters [ESI(+)]. The two ionization modes could be used complementary to differentiate components such as fatty acids [only ionisable in ESI(-)] and their corresponding isobaric ethyl esters [only ionisable in ESI(+)]. Samples were flow-injected straight forward in the ESI using a Hamilton 250 μ L syringe with a simple syringe injection pump at 0.12 mL/h.

- 8. Péron N, et al. (2001) Layers of macromolecules at the champagne/air interface and the stability of champagne bubbles. *Langmuir* 17:791–797.
- Péron N, Meunier J, Cagna A, Valade M, Douillard R (2004) Phase separation in molecular layers of macromolecules at the champagne-air interface. J Microscopy 214:89–98.
- Polidori G, Beaumont F, Jeandet P, Liger-Belair G (2008) Artificial bubble nucleation in engraved champagne glasses. J Visualization 11:279.
- 11. Liger-Belair G, Lemaresquier H, Robillard B, Duteurtre B, Jeandet P (2001) The secrets of fizz in champagne wines: A phenomenological study. *Am J Enol Vitic* 52:98 02
- Rossello-Mora R, et al. (2008) Metabolic evidences of biogeographic isolation of the extremophilic bacterium Salinibacter ruber. ISME J 2:242–253.
- 13. Wu Z, Rodgers RP, Marshall AG (2004) Two- and three- dimensional van Krevelen diagrams: A graphical analysis complementary to the Kendrick mass plot for sorting elemental compositions of complex organic mixtures based on ultrahigh-resolution broadband Fourier transform ion cyclotron resonance mass measurements. Anal Chem 76:2511–2516.

- Gougeon RD, et al. (2009) The chemodiversity of wines can reveal a metabologeography expression of cooperage oak wood. Proc Natl Acad Sci USA 106:9174–9179.
- Pueyo E, Martin-Alvarez PJ, Polo MC (1995) Relationship between foam characteristics and chemical composition in wines and Cavas (sparkling wines). Am J Enol Vitic 46:518–524.
- Suhre K, Schmitt-Kopplin P (2008) MassTRIX: Mass translator into pathways. Nucleic Acids Res 36:W481–W484.
- 17. Fleet GH (2003) Yeast interactions and wine flavor. Int J Food Microbiol 86:11–22.
- Roufet M, Bayonove CL, Cordonnier RE (1987) Lipid composition of grapevine berries, Vitis vinifera L: Changes during maturation and localization in the berry (Translated from French). Vitis 26:85–97.
- 19. Clarke RJ, Baker J (2004) Wine Flavour Chemistry (Blackwell Publishing, Oxford).
- Escudero A, Etievant P (1999) Effect of antioxidants on the flavor characteristics and the gas chromatography/olfactometry profiles of Champagne extracts. J Agric Food Chem 47:3303–3308.
- 21. Li H, Tao Y-S, Wang H, Zhang L (2008) Impact odorants of Chardonnay dry white wine from Changli County (China). Eur Food Res Technol 227:287–292.
- Drawert F, Rapp A (1966) Contents of musts and wines. VII. Investigations for aroma compounds in wines and their biogenesis by gas chromatography (Translated from German). Vitis 5:351–376.
- Razungles AJ, Baumes RL, Dufour C, Sznaper CN, Bayonove CL (1998) Effect of sun exposure on carotenoids and C13-norisoprenoid glycosides in Syrah berries (Vitis vinifera L.). Sci Aliment 18:361–373.

- Dimitriadis E, Strauss CR, Wilson B, Williams PJ (1985) The actinidols: Nor-Isoprenold compounds in grapes, wines and spirits. *Phytochemistry* 24:767–770.
- Schneider R, Razungles A, Augier C, Baumes R (2001) Monoterpenic and norisoprenoidic glycoconjugates of Vitis vinifera L. cv. Melon B. as precursors of odorants in Muscadet wines. J Chrom A 936:145–157.
- Caven-Quantrill DJ, Buglass AJ (2008) Seasonal variation of flavor content of English vineyard grapes, determined by stir-bar sorptive extraction-gas chromatography-mass spectrometry. Flavour Fragr J 23:239–248.
- Pagot Y, Le Clainche A, Nicaud J-M, Wache Y, Belin J-M (1998) Peroxisomal β-oxidation activities and γ-decalactone production by the yeast Yarrowia lipolytica. Appl Microbiol Biotechnol 49:295–300.
- Bonnländer B, Baderschneider B, Messerer M, Winterhalter P (1998) Isolation of two novel terpenoid glucose esters from Riesling wine. J Agric Food Chem 46: 1474–1478.
- 29. Winterhalter P, Messerer M, Bonnländer B (1997) Isolation of the glucose ester of (E)-2,6-dimethyl-6-hydroxyocta-2,7-dienoic acid from Riesling wine. Vitis 36:55–56.
- Alonso GL, Salinas MR, Esteban-Infantes FJ, Sanchez-Fernandez MA (1996) Determination of safranal from saffron (*Crocus sativus* L.) by thermal desorption-gas chromatography. *J Agric Food Chem* 44:185–188.
- 31. Flamini R (2005) Some advances in the knowledge of grape, wine and distillates chemistry as achieved by mass spectrometry. *J Mass Spectrom* 40:705–713.